An Artificial Photosynthetic Antenna-Reaction Center Complex

Darius Kuciauskas,[†] Paul A. Liddell,[†] Su Lin,[†] Thomas E. Johnson,[‡,§] Steven J. Weghorn,[‡] Jonathan S. Lindsey,*[,‡] Ana L. Moore,*[,†] Thomas A. Moore,*[,†] and Devens Gust*[,†]

Contribution from the Department of Chemistry and Biochemistry, Arizona State University, Tempe, Arizona 85287, and Department of Chemistry, North Carolina State University, Raleigh, North Carolina 27695

Received April 19, 1999. Revised Manuscript Received June 22, 1999

Abstract: A model photosynthetic antenna consisting of four covalently linked zinc tetraarylporphyrins, $(P_{ZP})_3-P_{ZC}$, has been joined to a free base porphyrin-fullerene artificial photosynthetic reaction center, $P-C_{60}$, to form a $(P_{ZP})_3-P_{ZC}-PC_{60}$ hexad. As revealed by time-resolved absorption and emission studies, excitation of any peripheral zinc porphyrin moiety (P_{ZP}) in 2-methyltetrahydrofuran solution is followed by singlet−singlet energy transfer to the central zinc porphyrin to give $(P_{ZP})_3-{}^1P_{ZC}-P-C_{60}$ with a time constant of ∼50 ps. The excitation is passed on to the free base porphyrin in 240 ps to produce $(P_{ZP})_3-P_{ZC}-{}^1P-C_{60}$, which decays by electron transfer to the fullerene with a time constant of 3 ps. The $(P_{ZP})_3-P_{ZC}-P^{\bullet+}-C_{60}^{\bullet-}$ charge-separated state thus formed has a lifetime of 1330 ps, and is generated with a quantum yield of 0.70 based on light absorbed by the zinc porphyrin antenna. The complex thus mimics the basic functions of natural photosynthetic antenna systems and reaction center complexes.

Introduction

Conversion of light to chemical potential energy in photosynthesis involves two basic photochemical processes. Light of the appropriate wavelengths is absorbed by ensembles of light-harvesting chromophores, and the resulting electronic excitation energy powers photoinduced electron transfer, generating an energetic charge-separated state. These two functions are carried out by different pigment−protein complexes associated with lipid bilayer membranes. Antenna systems consist of chromophore arrays that absorb light and transport the resulting excitation energy spatially to photosynthetic reaction centers. The transport mechanism is singlet−singlet energy transfer among the chromophores. Antenna structures vary from organism to organism and are optimized for the quality of light in a particular environment. The antenna is efficiently coupled to the reaction center pigments that are the ultimate energy acceptors; photosynthetic reaction centers directly absorb only a small fraction of the total light energy. The reaction center converts electronic excitation energy to chemical energy in the form of long-lived transmembrane charge separation via multistep photoinduced electron-transfer reactions. This electrochemical energy is later converted to other forms of biologically useful energy such as proton motive force.

It is possible to mimic the basic photochemistry of photosynthetic reaction centers using synthetic molecular constructs. Examples are porphyrin-based assemblies bearing covalently linked electron acceptors such as quinones, aromatic imides, fullerenes, and other porphyrins and/or electron donor moieties such as amines, porphyrins, or carotenoid polyenes.[1−8] Excitation of a porphyrin moiety of these molecules is followed by photoinduced electron transfer with a nearby donor or acceptor to generate a charge-separated state. In the more complex systems, this state may evolve by additional electron-transfer reactions that further separate the radical ions, thus increasing the lifetime of the charge separation. Systems of this type can rival natural photosynthesis with respect to quantum yield, fraction of energy stored, and charge separation lifetime.

Photosynthetic antenna function, which is based on singlet−singlet energy transfer among chromophores, can also be mimicked in artificial, covalently linked arrays. For example, metalated and free base porphyrins have been linked with alkyne units to form dimers, trimers, tetramers, pentamers, and more complex supermolecules that absorb light and rapidly and efficiently transfer singlet excitation to energy sinks such as a free base porphyrin moiety.[9−15] Some molecules of these types have been designed to act as photonic "wires"[16] and gates.[17]

[†] Arizona State University.
[‡] North Carolina State University.
[§] Current address: Department of Chemistry, University of Georgia, Athens, GA 30602.

(1) Gust, D.; Moore, T. A. *Adv. Photochem.* **1991**, *16*, 1−65.
(2) Gust, D.; Moore, T. A.; Moore, A. L. *Acc. Chem. Res.* **1993**, *26*, 198−205.
(3) Wasielewski, M. R. *Chem. Rev.* **1992**, *92*, 435−461.
(4) Bixon, M.; Fajer, J.; Feher, G.; Freed, J. H.; Gamliel, D.; Hoff, A. J.; Levanon, H.; Möbius, K.; Nechushtai, R.; Norris, J. R.; Scherz, A.; Sessler, J. L.; Stehlik, D. *Isr. J. Chem.* **1992**, *32*, 449−455.
(5) Asahi, T.; Ohkouchi, M.; Matsusaka, R.; Mataga, N.; Zhang, R. P.; Osuka, A.; Maruyama, K. *J. Am. Chem. Soc.* **1993**, *115*, 5665−5674.
(6) Connolly, J. S.; Bolton, J. R. In *Photoinduced Electron Transfer, Part D*; Fox, M. A., Chanon, M., Eds.; Elsevier: Amsterdam, The Netherlands, 1988; pp 303−393.
(7) Sakata, Y.; Imahori, H.; Tsue, H.; Higashida, S.; Akiyama, T.; Yoshizawa, E.; Aoki, M.; Yamada, K.; Hagiwara, K.; Taniguchi, S.; Okada, T. *Pure Appl. Chem.* **1997**, *69*, 1951−1956.
(8) Imahori, H.; Sakata, Y. *Adv. Mater.* **1997**, *9*, 537−546.
(9) Bothner-By, A. A.; Dadok, J.; Johnson, T. E.; Lindsey, J. S. *J. Phys. Chem.* **1996**, *100*, 17,551−17,557.
(10) Hsiao, J.-S.; Krueger, B. P.; Wagner, R. W.; Johnson, T. E.; Delaney, J. K.; Mauzerall, D. C.; Fleming, G. R.; Lindsey, J. S.; Bocian, D. F.; Donohoe, R. J. *J. Am. Chem. Soc.* **1996**, *118*, 11181−11193.
(11) Li, F.; Gentemann, S.; Kalsbeck, W. A.; Seth, J.; Lindsey, J. S.; Holten, D.; Bocian, D. F. *J. Mater. Chem.* **1997**, *7*, 1245−1262.
(12) Seth, J.; Palaniappan, V.; Johnson, T. E.; Prathapan, S.; Lindsey, J. S.; Bocian, D. F. *J. Am. Chem. Soc.* **1994**, *116*, 10578−10592.
(13) Seth, J.; Palaniappan, V.; Wagner, R. W.; Johnson, T. E.; Lindsey, J. S.; Bocian, D. F. *J. Am. Chem. Soc.* **1996**, *118*, 11194−11207.
(14) Strachan, J. P.; Gentemann, S.; Seth, J.; Kalsbeck, W. A.; Lindsey, J. S.; Holten, D.; Bocian, D. F. *J. Am. Chem. Soc.* **1997**, *119*, 11191−11201.

10.1021/ja991255j CCC: $18.00
Published on Web 09/01/1999

Other porphyrin arrays with demonstrated or potential antenna function have been reported.[18]

Given the progress made in mimicry of both photosynthetic antennas and reaction centers, a next step is to link an artificial light-harvesting array with a synthetic reaction center to produce a functional energy conversion complex. We report the synthesis and spectroscopic study of complex **1**, which features an antenna

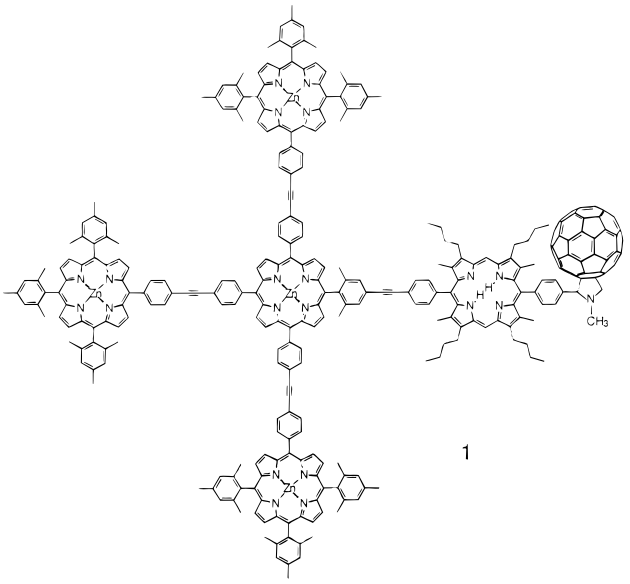

1

of four zinc porphyrin moieties, $(P_{ZP})_3-P_{ZC}$, linked to an artificial reaction center made up of a porphyrin electron donor joined to a fullerene acceptor ($P-C_{60}$). As described below, excitation of any zinc porphyrin of $(P_{ZP})_3-P_{ZC}-P-C_{60}$ is followed by singlet−singlet energy transfer to the free base porphyrin. The resulting excited state $(P_{ZP})_3-P_{ZC}-{}^1P-C_{60}$ donates an electron to the fullerene to generate an energetic charge-separated state, $(P_{ZP})_3-P_{ZC}-P^{\bullet+}-C_{60}{}^{\bullet-}$.

Results

Synthesis. The synthesis of zinc porphyrin antenna **2** and cleavage of the trimethylsilyl protecting group to give **7** will be reported elsewhere. Examination of the ^{1}H NMR spectra of **7** and related dimeric and trimeric porphyrin arrays revealed free rotation of the porphyrins about the ethyne and substantial bending of the diphenylethyne moiety.[9] Free base octa-alkyl-porphyrin **3** was synthesized from bis(3-butyl-4-methyl-2-pyrrolyl)methane, 4-bromobenzaldehyde, and 4-carbomethoxy-benzaldehyde using a modification of the MacDonald [2 + 2] cyclization,[19] as described in the Experimental Section. Palladium-induced coupling of **3** and **7** yielded **4**, a free base porphyrin bearing the antenna unit, and a carbomethoxy group. The latter was reduced to the benzyl alcohol using lithium aluminum hydride and then oxidized to the aldehyde with manganese dioxide to give **8**. Reaction[20] of **8**, C_{60}, and sarcosine gave **1**. Such reactions are known to produce only a single

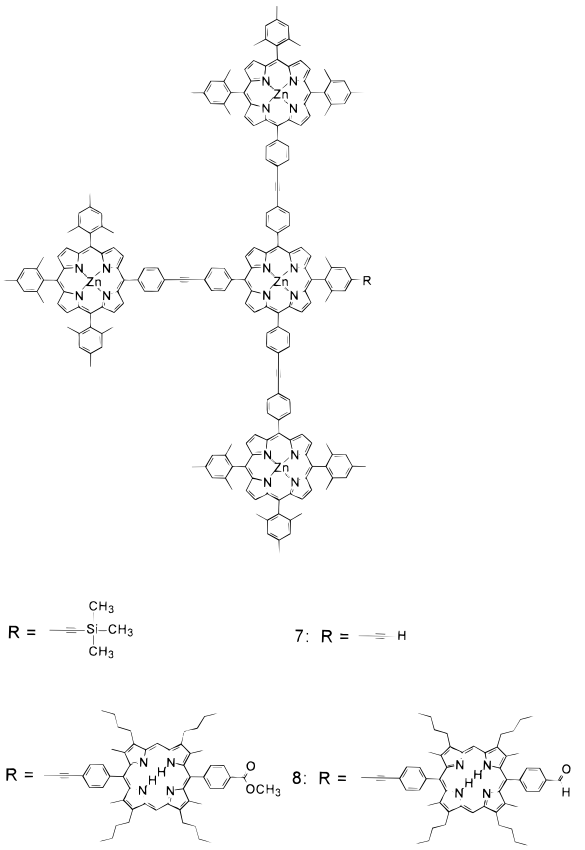

2: R = Si(CH$_3$)$_3$ 7: R = H

4: R = CO$_2$CH$_3$ 8: R = CHO

isomer; an adduct to a double bond at a 6,6-ring fusion in C_{60}.[20] Hexad **1** was characterized by NMR spectroscopy and mass spectrometry. As is the case with related antenna structures, **1** is soluble in many organic solvents to a greater extent than is necessary for the various spectroscopic measurements described below.

Absorption Spectra. The absorption spectrum of **1** in 2-methyltetrahydrofuran is shown in Figure 1. Absorption maxima are at 633 (sh), 599, 558, 508, 433, 425, and 300 nm. In addition, the long-wavelength maximum of the fullerene is observed at 705 nm, but its extinction coefficient is so low that it cannot be seen in the figure. As illustrated in the inset of Figure 1, the Q-band region of the porphyrins can be well approximated by a linear combination of the absorption spectra of zinc tetrad **2** (λ_{max} 602, 561, 520, 429, and 435 nm) and model free base porphyrin **6** (λ_{max} 633, 580, 541, 510, and 413 nm). In the Soret region, the free base porphyrin contributes only a small shoulder around 410 nm, and most of the absorption is due to the zinc porphyrins. The zinc porphyrin bands are excitonically split, as previously noted for similar zinc porphyrin arrays.[13] The Soret band of **1** is hypsochromically shifted from the corresponding band of **2** by ∼3 nm. The Soret band full width at half-maximum is 18.9 nm for **1** and 17.8 nm for **2**. The corresponding bandwidth for a model monomeric zinc porphyrin is 11.8 nm.[10]

The linear analysis of the absorption spectrum of **1** in terms of appropriate models shown in Figure 1 indicates that, although electronic interactions between the zinc porphyrins lead to perturbation of the Soret bands, the long-wavelength (Q-band) absorptions of all porphyrins and the fullerene are negligibly affected when the pigments are linked to form the array. In the point dipole approximation, exciton theory indicates that the interaction between chromophores should be inversely proportional to the cube of the interchromophoric distance and proportional to the square of the transition moments of the

(15) Wagner, R. W.; Johnson, T. E.; Lindsey, J. S. *J. Am. Chem. Soc.* **1996**, *118*, 11166−11180.
(16) Wagner, R. W.; Lindsey, J. S. *J. Am. Chem. Soc.* **1994**, *116*, 9759−9760.
(17) Wagner, R. W.; Lindsey, J. S.; Seth, J.; Palaniappan, V.; Bocian, D. F. *J. Am. Chem. Soc.* **1996**, *118*, 3996−3997.
(18) Van Patten, P.; Shreve, A. P.; Lindsey, J. S.; Donohoe, R. J. *J. Phys. Chem. B* **1998**, *102*, 4209−4216.
(19) Osuka, A.; Nagata, T.; Kobayashi, F.; Maruyama, K. *J. Heterocycl. Chem.* **1990**, *27*, 1657−1659.
(20) Maggini, M.; Scorrano, G.; Prato, M. *J. Am. Chem. Soc.* **1993**, *115*, 9798−9799.

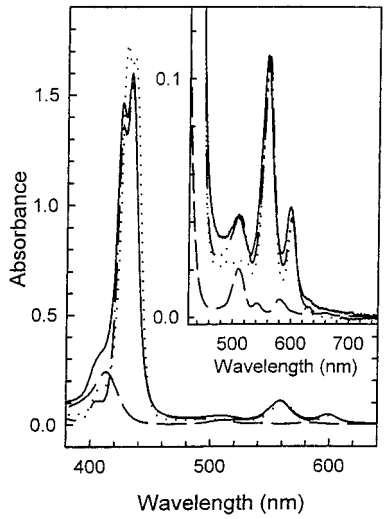

Figure 1. Absorption spectra in 2-methyltetrahydrofuran of hexad **1** (—), model antenna array **2** (···), model free base porphyrin **6** (- - -) and a linear combination of the spectra of **2** and **6** that approximates the spectrum of **1** (—··—). The inset is an expansion of the Q-band region.

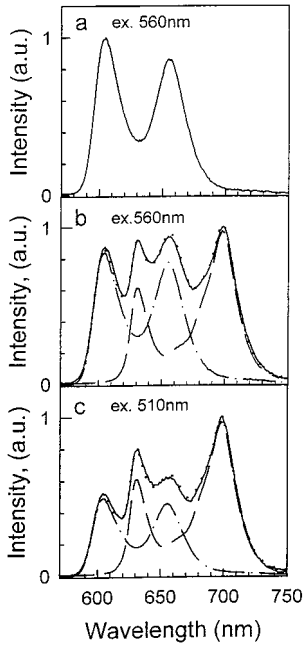

Figure 2. Fluorescence emission spectra in 2-methyltetrahydrofuran solution of hexad **1** with excitation at 560 nm (a) and model pentad **4** (solid line) and model compounds with excitation at 560 nm (b) and 510 nm (c), where the free base porphyrin moiety absorbs a greater fraction of the light. All spectra have been normalized to facilitate comparison of spectral shapes.

interacting chromophores. Thus, long-range exciton coupling in the zinc porphyrin arrays should only be seen for the high oscillator strength Soret bands and not for the weaker Q-bands, as is observed.[21,22]

The analysis of the absorption spectra also shows that it is possible to selectively excite the zinc porphyrin antenna at 560 nm or on the longer-wavelength side of the Soret band. Significant selectivity in excitation of the free base porphyrin may be achieved at 380−415 nm or at about 510 nm.

Fluorescence Emission. Figure 2a shows the fluorescence emission spectrum for **1** in 2-methyltetrahydrofuran with excitation at 560 nm, where most of the light is absorbed by the zinc porphyrin moieties. The emission spectrum features maxima at 605 and 654 nm (due to the Zn porphyrins), and very weak shoulders at ∼630 and 698 nm (due to the free base porphyrin). With the exception of these shoulders, the spectrum is nearly identical to that of antenna **2**, which also has maxima at 605 and 654 nm. Determination of the quantum yields shows that the emission for **1** ($\Phi_f = 0.0087$) is quenched by 3.7-fold relative to that of **2** ($\Phi_f = 0.032$).

More information concerning the nature of this quenching was obtained by measuring the emission spectrum of model pentad **4**, which lacks the fullerene moiety. Excitation at 560 nm yields an emission spectrum (Figure 2b) featuring not only the characteristic zinc porphyrin emission bands at 605 and 654 nm but also two new bands at 630 and 698 nm. The latter bands are characteristic of free base porphyrin **6**. The strong free base porphyrin emission following excitation at a wavelength where nearly all of the light is absorbed by the zinc porphyrin moieties suggests efficient singlet−singlet energy transfer from the zinc porphyrins to the free base. Excitation of **4** at 510 nm, where ∼47% of the light is absorbed by the free base porphyrin, yields a spectrum in which the free-base emission bands are more pronounced (Figure 2c). The presence of free base emission in **4** and its virtual absence in the spectrum of **1** suggest that the first excited singlet state of the free base porphyrin moiety of **1** is strongly quenched by the attached fullerene.

The emission spectra of model pentad **4** shown in Figure 2b,c are well approximated by a linear combination of the emission spectra of model tetrad **2** and model porphyrin **6**. This result supports the conclusion, based on the absorption spectra, that the porphyrin chromophores in **1**, **2**, and **4** are only weakly coupled in the lowest excited singlet state. In the case of excitation at 560 nm (Figure 2b), 51% of the emission is due to the zinc porphyrins, and 49% results from the free base porphyrin moiety. With 510 nm excitation (Figure 2c), 38% of the emission is due to the zinc porphyrins, whereas 62% comes from the free base. The fluorescence quantum yield of model porphyrin **6** in 2-methyltetrahydrofuran is 0.037. This yield, coupled with the fact that **4** contains four zinc porphyrin moieties and only one free base, contributes to the fact that free base and zinc porphyrin emission intensities are comparable in Figure 2, parts b and c, even though the zinc porphyrin moieties are quenched by singlet−singlet energy transfer (see also next section).

Time-Resolved Fluorescence. To probe the dynamics of the processes underlying the fluorescence quenching, we undertook time-resolved fluorescence experiments using the single-photon-timing technique. Excitation of a 2-methyltetrahydrofuran solution of zinc porphyrin array **2** at 600 nm and detection of fluorescence at 650 nm yielded a time profile that could be satisfactorily described by a single-exponential decay with a lifetime of 2.4 ns (Figure 3). This is similar to the fluorescence lifetime of monomeric zinc porphyrin model compounds.[10]

Hexad **1** was also excited at 600 nm, and the fluorescence decay was measured at 7 wavelengths in the 630−740 nm region. Global analysis of these data ($\chi^2 = 1.05$) yielded an exponential decay component with a lifetime of 700 ps, which makes up ≥95% of the decay. A second component with a lifetime of 2.4 ns (≤5% of the decay) was also required to fit the data; it is ascribed to a minor impurity. A typical decay (at 650 nm) is shown in Figure 3. The spectra of both decay components were similar to those of the zinc porphyrin, with

(21) Liang, K.; Farahat, M. S.; Perlstein, J.; Law; K.-Y.; Whitten, D. G. *J. Am. Chem. Soc.* **1997**, *119*, 830−831.

(22) McRae, E. G.; Kasha, M. *Physical Processes in Radiation Biology*; Academic Press: New York, 1964; p 17.

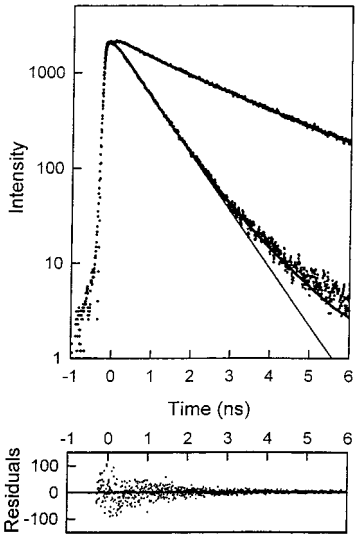

Figure 3. Fluorescence emission kinetics (log scale) for 2-methyltetrahydrofuran solutions of **1** (faster decay) and **2** (slower decay) measured at 650 nm following excitation at 600 nm. Shown as solid lines are the exponential fits obtained from the global analysis discussed in the text. Also shown is the result of a simulation of the normalized total excited-state population of the zinc porphyrin antenna of **1** based on the kinetic parameters discussed in the text (see also Figure 10). This simulation fits the major component of the decay for **1** at 650 nm very well. The second decay component, with an amplitude of ~5% and attributed to impurities, was not included in the simulation. The residuals shown at the bottom of the figure are for the global fitting results for hexad **1**.

maxima at ~600 and ~650 nm. The 700 ps decay is ascribed to the zinc porphyrin first excited singlet states by virtue of its spectrum. The significant shortening of the lifetimes of these states relative to that of the corresponding states in model compound **2** is ascribed to singlet−singlet energy transfer to the free base porphyrin, as also revealed by the steady-state emission spectra discussed above.

No significant emission from the free base porphyrin of **1** was observed in either time-resolved or steady-state experiments. This phenomenon was further investigated by exciting **1** at 580 nm, where ~25% of the light is absorbed by the free base porphyrin moiety. A global fit ($\chi^2 = 1.08$) of kinetic data taken at six wavelengths in the 610−825 nm region gave lifetimes identical to those measured with 600 nm excitation. Again, no emission from the free base porphyrin was detected. The lack of emission from the free base porphyrin is therefore due to very rapid quenching of $(P_{ZP})_3-P_{ZC}-{}^1P-C_{60}$, rather than to a failure to excite this moiety. The quenching is ascribed to photoinduced electron transfer to the fullerene (vide infra).

Similar experiments were carried out with model pentad **4**, which lacks the fullerene. The sample in 2-methyltetrahydrofuran was excited at 590 nm, and kinetics were measured at 7 wavelengths in the 610−735 nm region. Global analysis of these data as two exponential components ($\chi^2 = 1.12$) yielded lifetimes of 700 ps and 8.3 ns. The spectrum of the 700 ps component is very similar to that of **2**, and therefore, this component is due, for the most part, to the zinc porphyrin first excited singlet states. The correspondence of this lifetime with that observed in **1** indicates that these excited states are quenched by singlet−singlet energy transfer to the free base, as was noted for **1**. Indeed, analysis of the emission data at 720 nm, where the free base porphyrin emission is the main contributor (see Figure 2), shows that the 700 ps component has a small negative amplitude. The negative amplitude denotes a rise in fluorescence intensity with time and is ascribed to the rise of emission from the free base porphyrin moiety as a result of excitation transfer from the zinc porphyrin.

The 8.3 ns component of the fluorescence decay of **4** has the emission spectrum of a free-base porphyrin and, thus, represents the decay of $(P_{ZP})_3-P_{ZC}-{}^1P$. The lifetime of model porphyrin **6** in 2-methyltetrahydrofuran is 10.1 ns. The small decrease in free base porphyrin singlet lifetime in **4** could be due to small electronic perturbations resulting from the linking of the additional chromophores or to a small amount of singlet energy back-transfer from the free base into the zinc porphyrin antenna. On the basis of the absorption and emission spectra of **1** and model compounds, the free energy difference between the zinc and free base porphyrin singlet states is 0.09 eV. According to Boltzmann statistics at equilibrium at 292 K, the endergonic energy back-transfer rate from the free base porphyrin to the central zinc porphyrin should be about 0.03 times the forward, exergonic rate.

Time-Resolved Absorption. Transient absorption experiments were undertaken in order to better quantify the interconversions of the various excited states in these compounds and to allow detection of nonemissive states such as charge-separated species. A solution of **1** in 2-methyltetrahydrofuran was excited with ~100 fs laser pulses, and the transient absorption was recorded using the pump−probe method.

The sample was excited at 560 nm, where most of the light is absorbed by the zinc porphyrin moieties, and the spectrum was recorded in the 931−1065 nm region. A total of 61 kinetic traces were measured over this wavelength region, at times ranging from −50 to 450 ps relative to the laser flash. Representative spectral data at various times are shown in Figure 4a. In this wavelength region, absorptions of the fullerene radical anion, free base and metalated porphyrin first excited singlet states, and possibly the fullerene first excited singlet state might be expected. Perusal of Figure 4a shows no obvious distinct absorption bands.

The situation is clarified by a global analysis of the data. Singular value decomposition[23,24] shows that there are at least 3 significant kinetic components in the data. Decay-associated spectra were extracted by a three-exponential global fit of all 61 kinetic traces. The results are shown in Figure 5a. The shortest lifetime component (3 ps) is small and of negative amplitude throughout the region. In these spectra, a negative amplitude signifies a transient whose absorption is increasing (growing in) during the time period of observation. A second negative component of 12 ps is also observed. The final component, with a lifetime of 700 ps, has a positive amplitude, which signifies a decay of this component with time after the laser pulse. A typical example of a transient from which these decay-associated spectra were obtained is shown in Figure 6a. Superimposed upon the experimental data is the simulated data from the global fit. The rapid (12 ps) rise in absorption (corresponding to the negative amplitude in the decay-associated spectrum) is followed by the 700 ps decay. The amplitude of the 3 ps component is negligible at this wavelength.

The 700 ps decay component may be assigned to the zinc porphyrin excited singlet states, based on the time-resolved fluorescence results discussed above. The 3 ps component of the decay-associated spectrum is of particular interest, despite its relatively low amplitude. The inset in Figure 5a is an expansion of the spectrum of the 3 ps component. The apparent minimum at 995 nm, which corresponds to a grow-in of a

(23) Golub, G. H.; Reinsch, C. *Numer. Math.* **1970**, *14*, 403−420.
(24) Henry, E. R.; Hofrichter, J. In *Methods in Enzymology*; Ludwig, B., Ed.; Academic Press: San Diego, CA, 1992; p 219, Vol. 210.

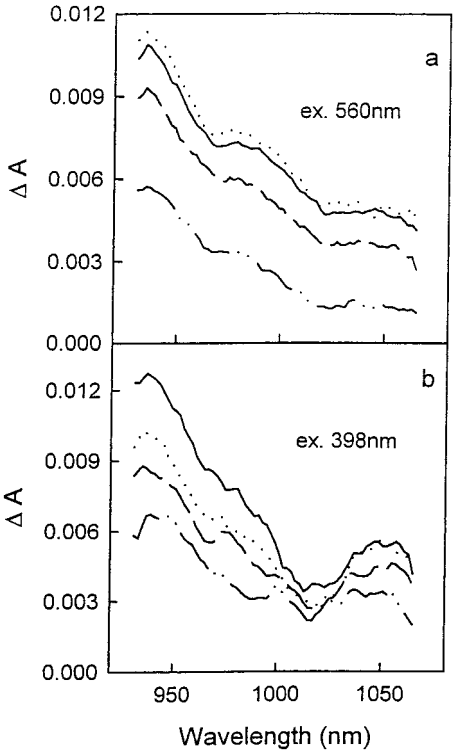

Figure 4. Transient absorption difference spectra measured for 2-methyltetrahydrofuran solutions of hexad **1** with excitation at 560 nm (a) and 398 nm (b). In a, the spectra were measured 20 ps (—), 60 ps (···), 170 ps (- - -), and 430 ps (—··—) after excitation. In b, spectra were determined at 15 ps (—), 55 ps (···), 145 ps (- - -), and 435 ps (—··—) after the laser flash. As discussed in the text, the zinc porphyrin, free base porphyrin first excited singlet states, and the charge-separated state all contribute to the transient absorption in this spectral region.

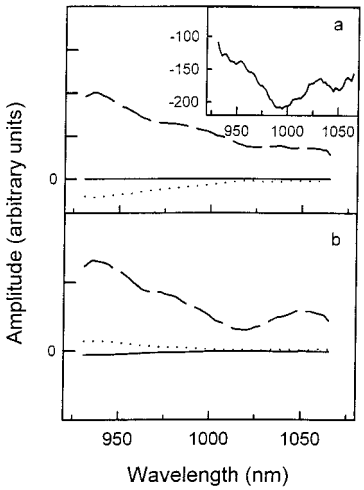

Figure 5. Decay-associated spectra for **1** in 2-methyltetrahydrofuran obtained from a global analysis of transient absorption data taken after excitation at 560 nm (a) and 398 nm (b). In a, the lifetimes of the components are 3 ps, (—), 12 ps (···), and 700 ps (- - -). The 3 ps component is enlarged in the inset. In b, the lifetimes are 3 ps, (—), 12 ps (···), and 1330 ps (- - -). In these decay-associated spectra, a component with a negative amplitude represents a transient that *increases* in intensity with time following excitation.

transient absorption, is characteristic of the fullerene radical anion. Thus, this transient is indicative of formation of the $(P_{ZP})_3-P_{ZC}-P^{\bullet+}-C_{60}^{\bullet-}$ charge-separated state from $(P_{ZP})_3-P_{ZC}-{}^1P-C_{60}$ with a 3 ps rise time.

Verification of the assignment of the absorption at 995 nm to the fullerene radical anion comes from a spectroscopic

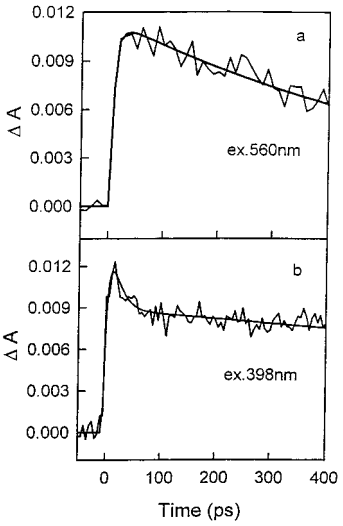

Figure 6. Transient absorption kinetics measured at 931 nm for hexad **1** in 2-methyltetrahydrofuran solution following laser excitation. The smooth curves are the results of global fits to all of the transient absorption data. With 560 nm excitation (a), the more rapid kinetic process has an associated time constant of 12 ps and a negative amplitude, signifying a rise in absorbance with time following the laser pulse. The slower decay can be fit with a lifetime of 700 ps. (Measurements on a longer time scale show that a 1330 ps component is also present (Figure 8)). With excitation at 398 nm (b), the more rapid kinetic process again has an associated time constant of 12 ps, but the amplitude is positive, signaling a decay of this transient following excitation. In this case, the long-lived decay may be fit with a lifetime of 1330 ps.

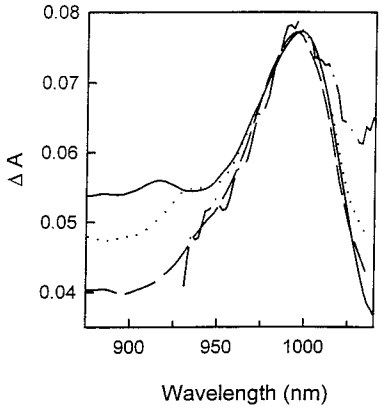

Figure 7. Transient absorption difference spectra for 2-methyltetrahydrofuran solutions of porphyrin—fullerene dyad **5** taken 100 ps following excitation at 590 nm. The spectra were taken at 292 K (—), 150 K (···), and 77 K (- - -). The maximum at ~1000 nm is due to the fullerene radical anion. Also shown (—·—) is the normalized spectrum of the 3 ps global decay component in Figure 5a, which has been inverted in order to appear in absorption mode.

investigation of porphyrin-fullerene dyad **5**. A 2-methyltetrahydrofuran solution of **5** was excited at 590 nm with 100 fs laser pulses, and its transient absorption spectrum was obtained as described for **1**. The spectra obtained 100 ps after excitation at various temperatures are shown in Figure 7. The exciting light is absorbed mainly by the porphyrin moiety, whose excited state decays with a time constant of 3 ps to yield the $P^{\bullet+}-C_{60}^{\bullet-}$ charge-separated state. This state can be readily identified by the fullerene radical anion absorption in the 1000 nm region. Superimposed on these spectra in Figure 7 is the spectrum of the 3 ps global decay component of **1** from Figure 5a, which has been inverted so as to appear in absorption mode and normalized to the other spectra. The identification of the

transient from **1** as due to $(P_{ZP})_3-P_{ZC}-P^{\bullet+}-C_{60}^{\bullet-}$ is made more certain by the fact that in both **1** and **5**, the charge-separated state is formed with a 3 ps time constant. In **5**, the charge-separated state decays to the ground state with a lifetime of 480 ps.

The identification of the 12 ps component of the decay-associated spectrum is more complex, as will be described below. Note that the fullerene first excited singlet state $(P_{ZP})_3-P_{ZC}-P-{}^1C_{60}$ does not contribute significantly to the spectra. The absorption of light by the fullerene at 560 nm is negligible in **1** (<1%). Also, the extremely rapid (3 ps) quenching of the free base porphyrin first excited singlet state of **1** and **5** by

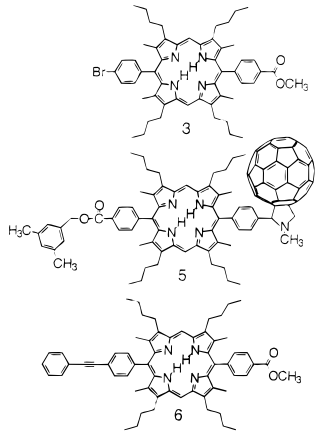

electron transfer to the fullerene means that significant singlet−singlet energy transfer from the free base porphyrin first excited singlet state to the fullerene is unlikely. This dominance of photoinduced electron transfer over singlet energy transfer in octa-alkylporphyrin-fullerene systems with the covalent linkage found in **1** and **5** has been noted previously.[8,25,26]

Measurements on longer time scales were undertaken in order to better define the longest lifetime in the decay-associated spectrum. Samples were excited at 560 nm and data collected as a function of time in the 900−1050 nm region. The decay at 931 nm observed over 3300 ps is shown in Figure 8. Also shown is a double-exponential fit to the data with lifetimes of 700 ps (36%) and 1330 ps (64%). The transient spectrum at 2750 ps features an absorption maximum at ∼1000 nm characteristic of the fullerene radical anion (cf. Figure 7), confirming the presence of the $(P_{ZP})_3-P_{ZC}-P^{\bullet+}-C_{60}^{\bullet-}$ charge-separated state as the longest-lived transient species.

As mentioned above, excitation at 560 nm gives mainly the zinc porphyrin excited singlet states. To gain more information about the role played by the free base porphyrin moiety and the nature of the 12 ps component, we also carried out transient absorption experiments with excitation at 398 nm, where a higher proportion of the light is absorbed by the free base porphyrin (Figure 1). Transient absorption data were recorded in the 931−1065 nm region at delay times ranging from −50 to 450 ps. Representative spectra at different times are shown in Figure 4b, and the decay-associated spectra resulting from singular value decomposition analysis appear in Figure 5b. The

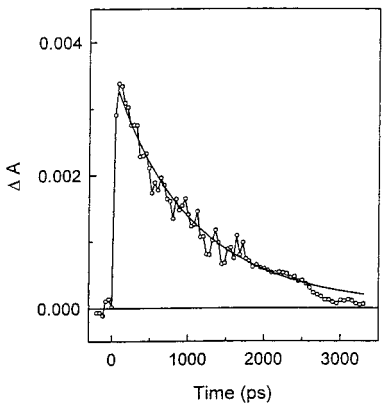

Figure 8. Transient absorption kinetics measured for hexad **1** in 2-methyltetrahydrofuran at 931 nm, following excitation at 560 nm. A two-exponential fit to the data with time constants of 700 ps (36%) and 1330 ps (64%) is shown as a smooth curve.

singular value decomposition showed that at least 3 exponential components were required. The lifetimes from global analysis are 3 ps (negative amplitude), 12 ps (positive amplitude), and 1330 ps (positive amplitude).

Because the 3 ps component is negative in amplitude, it represents an increase in absorption with time following excitation. It is again assigned to the formation of $(P_{ZP})_3-P_{ZC}-P^{\bullet+}-C_{60}^{\bullet-}$ from $(P_{ZP})_3-P_{ZC}-{}^1P-C_{60}$. The (negative) amplitude is larger at this excitation wavelength than with 560 nm excitation because a larger fraction of the light is directly absorbed by the free base porphyrin.

In distinction to the results with 560 nm excitation, the 12 ps component of the decay-associated spectrum is of positive amplitude with excitation at 398 nm. Thus, this transient absorption decays with time after excitation. This is clearly seen in Figure 6b, where the 12 ps decay component at 931 nm is followed by the 1330 ps decay. The fact that this 12 ps component appears as a decay with 398 nm excitation, where relatively more of the free base porphyrin is excited directly, and as a rise with 560 nm excitation, where relatively more of the zinc porphyrin is excited, suggests that it is associated with $(P_{ZP})_3-P_{ZC}-{}^1P-C_{60}$. This is also apparent in Figure 4, where the difference spectrum at 55 ps in Figure 4b has a significantly smaller amplitude than the spectrum at 15 ps, whereas the spectrum in Figure 4a at 60 ps has a slightly larger amplitude than the spectrum at 20 ps. To further bolster this assignment, we performed picosecond transient absorption experiments on model porphyrin **6** with 560 nm excitation. It was determined that **6** does indeed have excited-state absorption in the 900−1075 nm region. As discussed in the section on Analysis of Kinetic Data, this 12 ps component is a result of the interplay of several kinetic processes and is not a fundamental time constant for a single reaction.

Investigation of Triplet States. Although the major pathway for decay of the zinc porphyrin excited singlet states in **1** is singlet−singlet energy transfer, decay by the normal pathways of intersystem crossing, fluorescence, and internal conversion also occurs. The observation of electron-exchange-mediated singlet−singlet energy transfer in **1** suggests that related energy transfer phenomena might occur in the triplet manifold. Excitation of deoxygenated samples of **1** in 2-methyltetrahydrofuran with a ∼5 ns laser pulse at 560 nm permitted observation of several long-lived transients due to triplet states. One of these has a lifetime of 370 ns and was identified as the zinc porphyrin triplet state by virtue of absorption maxima at ∼450 nm and ∼840 nm. This state forms by normal intersystem crossing in

(25) Gust, D.; Moore, T. A.; Moore, A. L.; Liddell, P. A.; Kuciauskas, D.; Sumida, J. P.; Nash, B.; Nguyen, D. In *Recent Advances in the Chemistry and Physics of Fullerenes and Related Materials*; Kadish, K. M., Rutherford, A. W., Eds.; The Electrochemical Society: Pennington, NJ, 1997; pp 9−24, Vol. 4.

(26) Kuciauskas, D.; Liddell, P. A.; Moore, T. A.; Moore, A. L.; Gust, D. In *Recent Advances in the Chemistry and Physics of Fullerenes and Related Materials*; Kadish, K. M., Ruoff, R. S., Eds.; The Electrochemical Society: Pennington, NJ, 1998; pp 242−261, Vol. 6.

the zinc porphyrin antenna. A second transient with a lifetime of 10 μs features maxima at ~450 and 700 nm. These absorptions are characteristic of the free base porphyrin (450 nm)[27] and fullerene (700 nm)[25,28] triplets. Lifetimes measured at free base porphyrin and fullerene triplet maxima are identical.

The 370 ns lifetime of the zinc porphyrin triplet state is very short, as these states typically have lifetimes on the many microsecond time scale in deoxygenated solutions at ambient temperatures. Thus, a new pathway for decay of this species is present in multichromophoric **1**. It is postulated that the zinc porphyrin triplet states are quenched by triplet−triplet energy transfer to the lower-energy free base porphyrin to yield $(P_{ZP})_3-P_{ZC}-{}^3P-C_{60}$. This species in turn is in equilibrium with the fullerene triplet state, $(P_{ZP})_3-P_{ZC}-P-{}^3C_{60}$, via triplet−triplet energy transfer. This equilibrium is responsible for the observation that both $(P_{ZP})_3-P_{ZC}-{}^3P-C_{60}$ and $(P_{ZP})_3-P_{ZC}-P-{}^3C_{60}$ decay with the same lifetime. Similar triplet transfer and equilibria have been observed in other porphyrin-fullerene systems.[29−31]

Discussion

The design of functional artificial antenna-reaction center assemblies requires not only efficient light absorption by the antenna chromophores but also optimization of the yields of key energy and electron-transfer events that follow light absorption so that most of the absorbed photons lead to energy storage via charge separation. High yields demand in turn that the rate constants for the relevant energy and electron-transfer reactions be rapid relative to those for competing energy-wasting processes. To evaluate the performance of complex **1**, we must therefore extract rate constants from the steady-state and time-resolved spectroscopic data.

Kinetic Components. Although the photochemistry of multichromophoric **1** is necessarily complex, the combination of time-resolved fluorescence and absorption experiments has allowed the extraction of several lifetimes for kinetic processes. The time-resolved fluorescence and absorption data yield a time constant of 700 ps that is associated with the zinc porphyrin moieties. The shortening of the zinc porphyrin singlet lifetime from 2.4 ns in **2** to give a 700 ps component in **4** and **1** is a result of singlet−singlet energy transfer from the zinc porphyrins to the free base. In **1**, fluorescence from the free base porphyrin is quenched from its usual lifetime of ~10 ns to such a degree that fluorescence is no longer observable. The picosecond transient absorbance results yield additional time constants of 3, 12, and 1330 ps, regardless of whether excitation was at 560 or 398 nm.

Analysis of Kinetic Data. The model chosen for interpretation of the kinetic and spectroscopic data dealing with singlet energy and electron transfer in hexad **1** is shown in Figure 9. The energies of the various spectroscopic states were determined from the wavelength average of the longest-wavelength absorption and shortest-wavelength emission maxima of **1** and appropriate model compounds. The zinc porphyrin first excited

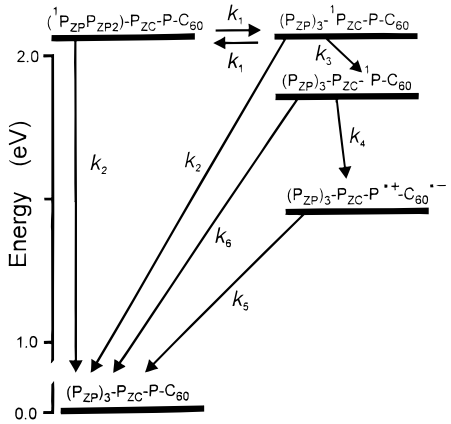

Figure 9. Transient states of hexad **1** and relevant interconversion pathways. The energies of the various states have been estimated as discussed in the text, and no correction for possible Coulombic effects on the energies of the charge-separated state has been made.

singlet states lie at 2.06 eV, whereas the energy of $(P_{ZP})_3-P_{ZC}-{}^1P-C_{60}$ is 1.96 eV above the ground state. The fullerene excited singlet state is not shown in the diagram, as the results show that this state was not significantly populated by either direct excitation or energy transfer in these experiments. The energy of the $(P_{ZP})_3-P_{ZC}-P^{\bullet+}-C_{60}^{\bullet-}$ charge-separated state was estimated as 1.43 eV, on the basis of the electrochemically determined oxidation potential of a model porphyrin (0.84 V vs SCE)[32] and reduction potential of a model fullerene (−0.59 V vs SCE).[33]

The following assumptions were made in the analysis:

(a) The four zinc porphyrin moieties of **1** are isoenergetic and equivalent in their inherent excited-state properties. The rate constants for singlet−singlet energy transfer among all four of these porphyrins are equal, with a value k_1. These assumptions are supported by the results of previous spectroscopic studies of closely related multiporphyrin arrays.[10]

(b) The rate constants for decay of each of the zinc porphyrin first excited singlet states by the usual photophysical pathways of fluorescence, intersystem crossing, and internal conversion are identical, and k_2 equals 4.2×10^8 s^{-1}, based on the 2.4 ns lifetime determined for model compound **2**. This is a typical lifetime for a zinc porphyrin of this type.

(c) Singlet−singlet energy transfer from $(P_{ZP})_3-{}^1P_{ZC}-P-C_{60}$ to the free base porphyrin, giving $(P_{ZP})_3-P_{ZC}-{}^1P-C_{60}$, occurs with a rate constant k_3. It is assumed that back energy transfer from the free base porphyrin to the zinc porphyrin antenna array is negligible ($\leq 0.03\ k_3$, as discussed above.) It is also assumed that the peripheral zinc porphyrin moieties transfer excitation only to the central zinc porphyrin and not directly to the free base porphyrin or directly to each other.

(d) The $(P_{ZP})_3-P_{ZC}-{}^1P-C_{60}$ excited state is quenched mainly by electron transfer to the fullerene moiety with a rate constant k_4. As discussed below, the short lifetime of $(P_{ZP})_3-P_{ZC}-{}^1P-C_{60}$ relative to the normal free base porphyrin excited-state lifetime of ~10 ns allows us to neglect k_6. In addition, singlet−singlet energy transfer from $(P_{ZP})_3-P_{ZC}-{}^1P-C_{60}$ to the fullerene is considered negligible, on the basis of results for **1** and model compound **5** and related dyads, as discussed above.

(e) Charge recombination of $(P_{ZP})_3-P_{ZC}-P^{\bullet+}-C_{60}^{\bullet-}$ occurs to yield the ground state with a rate constant k_5.

(27) Bonnett, R.; McGarvey, D. J.; Harriman, A.; Land, E. J.; Truscott, T. G.; Winfield, U.-J. *Photochem. Photobiol.* **1988**, *48*, 271−276.
(28) Williams, R. M.; Zwier, J. M.; Verhoeven, J. W. *J. Am. Chem. Soc.* **1995**, *117*, 4093−4099.
(29) Kuciauskas, D.; Lin, S.; Seely, G. R.; Moore, A. L.; Moore, T. A.; Gust, D.; Drovetskaya, T.; Reed, C. A.; Boyd, P. D. W. *J. Phys. Chem.* **1996**, *100*, 15926−15932.
(30) Liddell, P. A.; Sumida, J. P.; Macpherson, A. N.; Noss, L.; Seely, G. R.; Clark, K. N.; Moore, A. L.; Moore, T. A.; Gust, D. *Photochem. Photobiol.* **1994**, *60*, 537−541.
(31) Gust, D.; Moore, T. A.; Moore, A. L.; Kuciauskas, D.; Liddell, P. A.; Halbert, B. D. *J. Photochem. Photobiol., B* **1998**, *43*, 209−216.
(32) Kuciauskas, D.; Liddell, P. A.; Hung, S.-C.; Lin, S.; Stone, S.; Seely, G. R.; Moore, A. L.; Moore, T. A.; Gust, D. *J. Phys. Chem.* **1997**, *101*, 429−440.
(33) Maggini, M.; Karlsson, A.; Scorrano, G.; Sandona, G.; Farina, G.; Prato, M. *J. Chem. Soc., Chem. Commun.* **1994**, 589−590.

(f) Multiple excitations of pigments are not considered.

Given these assumptions, the singlet energy and electron-transfer processes in **1** are described by the following set of first-order linear differential equations.

$$\frac{d[^1P_{ZP}]}{dt} = -(k_1 + k_2)[^1P_{ZP}] + k_1[^1P_{ZC}] \quad (1)$$

$$\frac{d[^1P_{ZC}]}{dt} = -(3k_1 + k_3 + k_2)[^1P_{ZC}] + 3k_1[^1P_{ZP}] \quad (2)$$

$$\frac{d[^1P]}{dt} = -k_4[^1P] + k_3[^1P_{ZC}] \quad (3)$$

$$\frac{d[P^{\bullet+}C_{60}^{\bullet-}]}{dt} = -k_5[P^{\bullet+}C_{60}^{\bullet-}] + k_4[^1P] \quad (4)$$

In these equations, $[^1P_{ZP}]$ represents the concentration of excited states of the peripheral zinc porphyrin moieties, $[^1P_{ZC}]$ is the concentration of excited states of the central zinc porphyrin $(P_{ZP})_3-{}^1P_{ZC}-P-C_{60}$, $[^1P]$ is the concentration of excited states of the free base porphyrin $(P_{ZP})_3-P_{ZC}-{}^1P-C_{60}$, and $[P^{\bullet+}C_{60}^{\bullet-}]$ is the concentration of molecules in the charge-separated state $(P_{ZP})_3-P_{ZC}-P^{\bullet+}-C_{60}^{\bullet-}$. It will be noted that, although only one equation is written for the three equivalent peripheral zinc porphyrins (eq 1), the absorption of all three must be taken into account when solving the equations numerically.

Solving eqs 1−4 for the concentrations of the relevant species gives the following results.

$$[^1P_Z] = a_1e^{-\alpha_1 t} + a_2e^{-\alpha_2 t} \quad (5)$$

$$[^1P] = a_3e^{-k_4 t} + a_4e^{-\alpha_1 t} + a_5e^{-\alpha_2 t} \quad (6)$$

$$[P^{\bullet+}C_{60}^{\bullet-}] = a_6e^{-k_5 t} + a_7e^{-k_4 t} + a_8e^{-\alpha_1 t} + a_9e^{-\alpha_2 t} \quad (7)$$

$$\alpha_{1,2} = \frac{4k_1 + k_3 + 2k_2}{2} \pm \frac{1}{2}\sqrt{k_3^2 + 4k_1k_3 + 16k_1^2} \quad (8)$$

In these equations, only the total concentration of zinc porphyrin first excited singlet state, $[^1P_Z] = 3[^1P_{ZP}] + [^1P_{ZC}]$, is given, since all four zinc porphyrins are spectroscopically indistinguishable. The α_1 and α_2 values are phenomenological rate constants that would be observed experimentally. The a_i values are amplitudes. As seen in eqs 5−8, rate constants will not depend on either the excitation or the measurement wavelengths.

It will be noted from eqs 6 and 7 that the rate constant for photoinduced electron transfer k_4 and the charge recombination rate constant k_5 will be directly observed experimentally. As discussed in the Results section, k_4 equals the reciprocal of the 3 ps time constant detected in the transient absorption experiments, or 3×10^{11} s^{-1}. This assignment is verified by the results for model P−C_{60} dyad **5**, where the same value was obtained for the rate constant for photoinduced electron transfer. The charge recombination of $(P_{ZP})_3-P_{ZC}-P^{\bullet+}-C_{60}^{\bullet-}$ is associated with the 1330 ps decay component observed in transient absorption, as demonstrated by the spectral signature of the fullerene radical anion in this transient. There are several other arguments that support this assignment. In the first place, the fluorescence results show that none of the excited singlet states have such a long lifetime. Fluorescence from the zinc porphyrin moieties decays with a time constant of 700 ps. The free base porphyrin first excited singlet state is quenched to 3 ps. The fullerene first excited singlet state was not significantly populated in this experiment, and no emission from this state was observed in **1** or in model dyad **5**. In addition, triplet states of the three different kinds of chromophores were observed and have lifetimes on the hundreds of nanoseconds or miscoseconds time scales. These results suggest by elimination that the 1330 ps lifetime is that of $(P_{ZP})_3-P_{ZC}-P^{\bullet+}-C_{60}^{\bullet-}$. This lifetime is within a factor of 2.5 of the lifetime observed for $P^{\bullet+}-C_{60}^{\bullet-}$ in dyad **5** (480 ps).

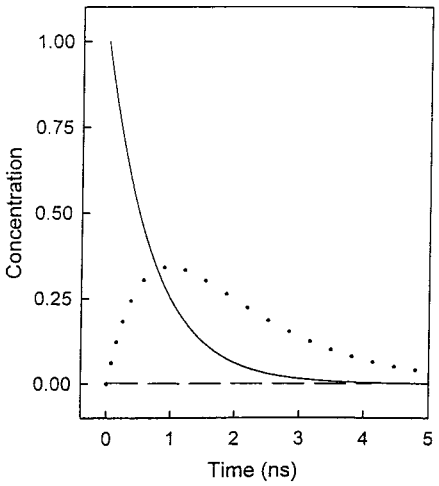

Figure 10. Simulation of the time course of the populations of zinc porphyrin first excited singlet states (—), the free base porphyrin first excited singlet state (- - -), and the $(P_{ZP})_3-P_{ZC}-P^{\bullet+}-C_{60}^{\bullet-}$ charge-separated state (···) of hexad **1** following excitation of only the zinc porphyrin antenna system. The rate constants used in the simulation are those derived from the kinetic analysis of the experimental data, as discussed in the text. All populations are relative to an initial concentration of 1.00 for the zinc porphyrin excited states. These simulation results are excellent fits to the experimental data (see, for example, Figure 3).

Having values for the electron-transfer rate constants k_4 and k_5, values for the singlet energy-transfer rate constants k_1 and k_3 are needed. The corresponding time constants do not appear directly in the experimental decays, which give α_1 and α_2 instead. Experimentally, α_1 and α_2 can be assigned values of 8.3×10^{10} and 1.4×10^9 s^{-1} from the measured lifetimes of 12 and 700 ps. Solving eq 8 using these values and that for k_2 given above yields values of 2.0×10^{10} s^{-1} for k_1 and 4.1×10^9 s^{-1} for k_3. The values thus obtained are predicated upon the validity of assumptions *a*−*f* and subject to error due to the random noise in the kinetic traces, but that for k_1 is in excellent agreement with the results of Hsiao and co-workers,[10] who measured a rate constant of 1.9×10^{10} s^{-1} for singlet energy transfer between two zinc porphyrins in a linear trimeric array with zinc porphyrin substituents and diphenylethyne linkages very similar to those in **1**.

Thus, it is possible to extract all of the relevant rate constants in Figure 9 from the experimental data. Figure 10 shows a simulation of the kinetic pathways in Figure 9 using the rate constants given above and assuming excitation only into the zinc porphyrin antenna system. The simulation for the decay of the zinc porphyrin excited states agrees very well with the experimentally measured 700 ps exponential decay of zinc porphyrin fluorescence shown in Figure 3. With excitation of only the zinc porphyrin moieties, the concentration of $(P_{ZP})_3-P_{ZC}-{}^1P-C_{60}$ is always very small.

Quantum Yield. The quantum yield of $(P_{ZP})_3-P_{ZC}-P^{\bullet+}-C_{60}^{\bullet-}$ will be wavelength-dependent. On the basis of light absorbed by the free base porphyrin, the yield is unity, due to the very large rate constant for photoinduced electron transfer,

k_4. The quantum yield based on excitation of the zinc porphyrins in the antennas may be determined numerically by assuming that k_5 in eq 4 is zero and integrating the total concentration of the charge-separated state. This calculation gives a quantum yield of 0.69.

Energy-Transfer Mechanism. The zinc porphyrin moieties of **1** serve as efficient antennas for the free base porphyrin, which initiates photoinduced electron transfer. Effective antenna function requires both a large absorption cross section for the antenna chromophores at the wavelengths of interest and efficient singlet−singlet energy transfer between these chromophores and the reaction center, where electron transfer occurs. We have previously shown that the energy-transfer process in diphenylethyne-linked porphyrin arrays involves a large contribution from a through-bond mechanism and a small contribution from a through-space mechanism. Thus the observed rate of transfer (k_{trans}) represents the sum of the rates for through-bond (k_{TB}) and through-space (k_{TS}) transfer (eq 9).

$$k_{trans} = k_{TB} + k_{TS} \tag{9}$$

$$\chi_{TB} = k_{TB}/k_{trans} \tag{10}$$

$$\chi_{TB} + \chi_{TS} = 1 \tag{11}$$

The through-space mechanism involves the Förster through-space resonant interaction of the transition dipoles of the respective porphyrins.[34,35] The rate of Förster singlet−singlet energy transfer from $(P_{ZP})_3-{}^1P_{ZC}-P-C_{60}$ to yield $(P_{ZP})_3-P_{ZC}-{}^1P-C_{60}$ is calculated[36,37] to be $k_{TS} = 6.7 \times 10^8\ s^{-1}$. The measured rate constant for this singlet transfer, k_3, is $4.1 \times 10^9\ s^{-1}$. Thus, the through-bond energy-transfer rate is inferred to be $k_{TB} = 3.4 \times 10^9\ s^{-1}$. The through-bond rate is 5 times faster than the through-space rate, and the through-bond mechanism makes a significant contribution ($\chi_{TB} = 0.83$) to the overall energy-transfer process. A through-bond mechanism has been implicated in other diphenylethyne-linked porphyrin arrays[10,14] as well as amide-linked architectures.[38]

The effective coupling of antenna and reaction center units is essential for efficient energy conversion. In this context, the question arose as to why the rate of transfer between the central zinc porphyrin in the antenna of **1** and the free base porphyrin was slow ($240\ ps^{-1}$) compared with that among the zinc porphyrins ($50\ ps^{-1}$). One possible explanation involves the frontier molecular orbitals in the two types of porphyrins. We have found that the nature of the frontier molecular orbitals can significantly alter the rate of through-bond energy transfer.[14,39,40] The HOMOs of porphyrins are either the a_{2u} orbital, which has lobes at the meso positions, or the a_{1u} orbital, which has nodes at the meso positions. Meso-linked arrays comprised of porphyrins with a_{2u} HOMOs undergo rapid energy transfer, whereas similar arrays comprised of porphyrins with a_{1u} HOMOs undergo much slower energy transfer. A rate difference of 10-fold has been attributed to such orbital ordering effects. The insight into these orbital ordering effects was prompted by the observation that meso-linked porphyrins bearing eight β-alkyl substituents exhibit substantially slower (17-fold) energy-transfer rates than their β-unsubstituted counterparts. The presence of the eight β-alkyl substituents is believed to result in the a_{1u} HOMO and thereby give a diminished through-bond energy-transfer rate. In molecules with β substituents, the rate can be further diminished by a sterically induced decrease in the dihedral angle between the planes of the porphyrin ring and *meso*-aryl ring, which in turn diminishes the $\pi-\pi$ contribution to through-bond transfer. In **1** the porphyrins in the antenna have meso but no β substituents, while the free base porphyrin in the reaction center has eight β and two meso substituents. Singlet−singlet energy transfer from a zinc tetraarylporphyrin to a free base tetraarylporphyrin covalently linked via a dimethyl-substituted diphenylethyne linker similar to that in **1** was dominated by a through-bond mechanism ($\chi_{TB} = 0.93$), where the rate of TB transfer was 14 times faster than the rate of TS transfer. The lesser contribution of the TB mechanism and comparatively slower overall rate of transfer from the zinc porphyrin to the free base porphyrin in **1** is likely due to a large extent to the presence of the a_{1u} HOMO in the free base porphyrin. Other antenna−reaction center complexes are currently being synthesized to test this conjecture.

Location of the Radical Cation. In the above discussion, the charge-separated state formed in **1** has been represented as $(P_{ZP})_3-P_{ZC}-P^{\bullet+}-C_{60}^{\bullet-}$. The first oxidation potentials of models for the free base octa-alkylporphyrin and zinc tetra-arylporphyrin moieties of **1** are nearly identical. Thus, the $(P_{ZP})_3-P_{ZC}-P^{\bullet+}-C_{60}^{\bullet-}$ state initially formed by photoinduced electron transfer might subsequently evolve into or equilibrate with states in which the radical cation resides on one of the zinc porphyrins. The spectral data obtained for **1** did not allow determination of the location of the radical cation, and so these possible charge-separated states were not included in the analysis above. The fact that the lifetime of the charge-separated state in **1** is about twice that in dyad **5** might be taken as evidence for such charge migration. However, the effect is relatively small.

Although the lifetime of $(P_{ZP})_3-P_{ZC}-P^{\bullet+}-C_{60}^{\bullet-}$ is longer than that of the corresponding state in **5**, it is considerably shorter than those observed for carotenoid−porphyrin−fullerene triads and other triad artificial reaction centers.[2,25] The shorter lifetime of the charge-separated state in the hexad is not inconsistent with migration of the radical cation to the zinc porphyrin array. Such hole-hopping has been observed in diphenylethyne-linked meso-substituted porphyrin arrays.[12,13] Additionally, since the zinc porphyrin and free base porphyrin radical cations are nearly isoenergetic, there would be no significant thermodynamic barrier to rapid equilibration of the radical cation among the various porphyrin centers and likewise no significant thermodynamic barrier to charge recombination. Vectorial charge migration to the zinc porphyrins could be encouraged by raising the oxidation potential of the free base porphyrin or lowering the oxidation potentials of the metalated porphyrins through changes in peripheral substitution or metal ion.

Conclusions

The results for **1** and associated model compounds demonstrate the natural intersection of two lines of artificial photo-

(34) Förster, T. *Ann. Phys.* **1948**, *2*, 55−75.
(35) Eyring, L. H.; Lin, S. H.; Lin, S. M. *Basic Chemical Kinetics*; John Wiley and Sons: New York, 1980; pp 289−297.
(36) The values used in this calculation are as follows: the orientation term $\kappa^2 = 1.125$, the refractive index for 2-methyltetrahydrofuran gives $n = 1.407$, the center-to-center distance between the porphyrins was taken as 20 Å, and the spectral values were obtained from the PhotochemCAD program.[37] The calculations gave a value for the overlap integral J of $1.2 \times 10^{-14}\ cm^6\ mmol^{-1}$ and a singlet energy-transfer rate constant of $6.7 \times 10^8\ s^{-1}$.
(37) Du, H.; Fuh, R.-C. A.; Li, J.; Corkan, A.; Lindsey, J. S. *Photochem. Photobiol.* **1998**, *68*, 141−142.
(38) Gust, D.; Moore, T. A.; Moore, A. L.; Makings, L. R.; Seely, G. R.; Ma, X. C.; Trier, T. T.; Gao, F. *J. Am. Chem. Soc.* **1988**, *110*, 7567−7569.
(39) Yang, S. I.; Seth, J.; Balasubramanian, T.; Kim, D.; Lindsey, J. S.; Holten, D.; Bocian, D. F. *J. Am. Chem. Soc.* **1999**, *121*, 4008−4018.
(40) Yang, S. I.; Seth, J.; Strachan, J. P.; Gentemann, S.; Kim, D.; Holten, D.; Lindsey, J. S.; Bocian, D. F. *J. Porphyrins Phthalocyanines* **1999**, *3*, 117−147.

synthetic research, wherein artificial reaction centers are mated to artificial antenna systems. Light gathered by the peripheral zinc porphyrins of **1** is transferred to the central zinc porphyrin to give $(P_{ZP})_3-{}^1P_{ZC}-P-C_{60}$ with a time constant of 50 ps. This state donates energy to the free base porphyrin of the artificial reaction center portion with a time constant of 240 ps to yield $(P_{ZP})_3-P_{ZC}-{}^1P-C_{60}$, which decays in 3 ps by photoinduced electron transfer to the fullerene, giving $(P_{ZP})_3-P_{ZC}-P^{\bullet+}-C_{60}^{\bullet-}$. The charge-separated state has a lifetime of ~1 ns. In this process, the light-gathering power of the system is increased tremendously at many wavelengths, as four zinc porphyrin moieties feed excitation energy to the reaction center (see the absorption spectra in Figure 1).

The results obtained with this antenna−reaction center system point to several areas for further optimization. For example, the overall energy-transfer efficiency from the zinc porphyrins is ~0.7. The efficiency is limited by k_1 and k_3, which are too small to minimize losses due to decay of the zinc porphyrin excited states by k_2. The importance of the magnitude of k_1 cannot be overemphasized. For example, a P_Z-P-C_{60} triad with energy and electron-transfer rate constants equal to those for similar processes in **1** would have an overall quantum yield for charge separation of 0.91, based on light absorbed by the zinc porphyrin; the increased yield is due to the lack of energy-draining steps k_2 in the three extra antenna porphyrins of **1**. Potential strategies for increasing the energy-transfer yield include (1) replacement of the zinc porphyrins with magnesium porphyrins which have diminished k_2,[11] (2) use of shorter linkers to achieve increases in k_1,[41] and (3) optimal matching of the site of linker connection, frontier molecular orbitals,[39,40] and steric factors for enhanced through-bond energy transfer. In addition, tuning of redox potentials and/or addition of new donor and acceptor moieties would allow migration of the electrons and/or holes to create longer-lived charge-separated states. A logical extension of this work will be to increase the size of the zinc porphyrin arrays in order to harvest even more light for each reaction center. In these systems, extremely rapid inter-porphyrin singlet−singlet energy transfer will be necessary if substantial quantum yields are to be achieved. The design considerations affecting the performance of large antenna systems have been recently discussed.[18]

Experimental Section

(1) Synthesis. (A) 5-(4-Bromophenyl)-15-(4-carbomethoxyphenyl)-2,8,12,18-tetrabutyl-3,7,13,17-tetramethylporphyrin (3) was prepared from bis(4-butyl-3-methyl-2-pyrrol)methane, 4-carbomethoxybenzaldehyde, and 4-bromobenzaldehyde using the method of Maruyama and co-workers.[19] Porphyrin 3 was obtained in 35% yield: ^{1}H NMR (300 MHz, $CDCl_3$) δ −2.41 (2 H, s, NH), 1.10 (12 H, t, J = 7 Hz, CH_3), 1.75 (8 H, m, CH_2), 2.17 (8 H, m, CH_2), 2.46 (6 H, s, CH_3), 2.51 (6 H, s, CH_3), 3.98 (8 H, t, J = 7 Hz, CH_2), 4.14 (3 H, s, CO_2CH_3), 7.88 (2 H, d, J = 8 Hz, 15 Ar−H), 7.93 (2 H, d, J = 8 Hz, 15 Ar−H), 8.18 (2 H, d, J = 8 Hz, 5 Ar−H), 8.44 (2 H, d, J = 8 Hz, 5 Ar−H), 10.25 (2 H, s, meso H); MALDI-TOF-MS *m*/*z* calcd for $C_{54}H_{63}N_4BrO_2$ 878, obsd 879; UV/vis (CH_2Cl_2) 408, 508, 542, 576, 628 nm.

(B) 15-(4-(2-(Phenylethynyl)phenyl))-5-(4-carbomethoxyphenyl)-2,8,12,18,-tetrabutyl-3,7,13,17-tetramethylporphyrin (6). To a Schlenk tube was added 100 mg (0.114 mmol) of porphyrin **(3)**, 20 mL of triethylamine, and 19 μL (0.170 mmol) of phenylacetylene. The solution was cooled to −15 °C, and the suspension was flushed with argon for 30 min. Tetrakis(triphenylphosphine)palladium (0) (13 mg, 0.014 mmol) was added to the reaction mixture, and the argon stream was continued for an additional 20 min. The tube was sealed, and the contents were warmed to 80 °C with stirring for 24 h. After cooling, the reaction mixture was diluted with methylene chloride and washed with 0.5 M citric acid and then with aqueous sodium bicarbonate. The solvent was evaporated, and the residue was chromatographed on silica gel (methylene chloride/hexanes) to give 76 mg of **6** (74% yield): ^{1}H NMR (300 MHz, $CDCl_3$) δ −2.37 (2 H, s, NH), 1.10 (12 H, t, J = 8 Hz, CH_3), 1.75 (8 H, m, CH_2), 2.17 (8 H, m, CH_2), 2.46 (6 H, s, CH_3), 2.55 (6 H, s, CH_3), 3.99 (8 H, m, CH_2), 4.14 (3 H, s, CO_2CH_3), 7.20−7.50 (3 H, m, Ar−H), 7.71−7.74 (2 H, m, Ar−H), 7.94 (2 H, d, J = 8 Hz, 15Ar−H), 8.07 (2 H, d, J = 8 Hz, 15Ar−H), 8.19 (2 H, d, J = 8 Hz, 5Ar−H), 8.44 (2 H, d, J = 8 Hz, 5Ar−H); FAB-MS *m*/*z* calcd for $C_{62}H_{68}N_4O_2$ 901, obsd 902 $(M + 1)^+$; UV/vis (CH_2Cl_2) 408, 508, 542, 576, 628 nm.

(C) Porphyrin-C_{60} Dyad 5. Compound **5** was prepared as reported previously for a closely related dyad.[42] The synthesis and characterization of **5** will be reported in detail at a later date.

(D) Pentad Ester 4. To a Schlenk tube was added 25 mg (7.8×10^{-6}mol) of tetrad **7**, 7 mg (7.8×10^{-6} mol) of porphyrin **3**, and 10 mL of triethylamine. The resulting pink solution was cooled to −15 °C, and argon was bubbled through it for 20 min. Tetrakis(triphenylphosphine)palladium (0) (1 mg, 8×10^{-7} mol) was added to the reaction mixture, and bubbling was resumed for an additional 20 min. The tube was then sealed and heated to 80 °C with stirring for 24 h. The reaction mixture was concentrated under vacuum, and the residue was chromatographed on silica gel (methylene chloride/hexanes 1:1 to 5:1) to give 10 mg (32% yield) of the desired pentad **4**: ^{1}H NMR (500 MHz, $CDCl_3$) δ −2.34 (2 H, s, NH), 1.12 (6 H, t, J = 7 Hz, CH_3), 1.14 (6 H, t, J = 7 Hz, CH_3), 1.74−1.82 (8 H, m CH_2), 1.88 (54 H, s, Ar−oCH_3), 2.05 (6 H, s, Ar−oCH_3), 2.18−2.24 (8 H, m, CH_2), 2.48 (6 H, s, CH_3, P), 2.63 (6 H, s, CH_3, P), 2.65 (27 H, s, Ar−pCH_3), 4.01−4.04 (8 H, m CH_2), 4.13 (3 H, s, CO_2CH_3), 7.28 (6 H, s, Ar−H), 7.30 (12 H, s, Ar−H), 7.93 (2 H, s, Ar−H), 8.11 (8 H, d, J = 8 Hz, Ar−H), 8.15 (4 H, d, J = 8 Hz, Ar−H), 8.18 (4 H, d, J = 8 Hz, Ar−H), 8.21 (4 H, d, J = 8 Hz, Ar−H), 8.33 (6 H, d, J = 8 Hz, Ar−H), 8.38 (2 H, d, J = 9 Hz, Ar−H), 8.40 (4 H, d, J = 9 Hz, Ar−H), 8.44 (2 H, d, J = 9 Hz, Ar−H), 8.73 (12 H, s, β-H), 8.83 (6 H, d, J = 5 Hz, β-H), 8.97 (6 H, d, J = 5 Hz, β-H), 8.98 (2 H, d, J = 5 Hz, β-H), 9.13 (2 H, d, J = 5 Hz, β-H), 9.15 (4 H, s, β-H), 10.29 (2 H, s, meso-H); MALDI-TOF-MS *m*/*z* calcd for $C_{267}H_{226}N_{20}O_2Zn_4$ 4008, obsd 4009; UV/vis (CH_2Cl_2) 422, 428, 518, 552, 590, 623 nm.

(E) Pentad Aldehyde 8. Pentad ester **4** (8 mg, 2×10^{-6} mol) was dissolved in 8 mL of tetrahydrofuran and cooled to −15 °C. Sufficient lithium aluminum hydride was then added to the reaction mixture to bring about the reduction of the ester. Once all of the starting material had been consumed, as established by TLC analysis, the reaction mixture was diluted with methylene chloride and washed with water. After drying the organic solution over anhydrous sodium sulfate, the solvent was evaporated. The residue was redissolved in methylene chloride (12 mL), and manganese dioxide was added in small portions at 10 min intervals. After 30 min, TLC indicated that the alcohol had been converted to a less polar compound. The reaction mixture was filtered through Celite, and the residue was washed thoroughly with methylene chloride/methanol (2:1). The filtrate was concentrated and the residue was chromatographed on silica gel (methylene chloride/0.2% acetone) to give 7 mg (88% yield) of the desired aldehyde **8**: ^{1}H NMR (500 MHz,$CDCl_3$) δ −2.34 (2 H, s, NH), 1.12 (6 H, t, J = 8 Hz, CH_3), 1.14 (6 H, t, J = 8 Hz, CH_3), 1.74−1.80 (8 H, m, CH_2), 1.88 (54 H, s, Ar−oCH_3), 2.05 (6 H, s, Ar−oCH_3), 2.17−2.24 (8 H, m, CH_2), 2.48 (6 H, s, CH_3,P), 2.64 (6 H, s, CH_3,P), 2.65 (27 H, s, Ar−pCH_3), 3.99−4.06 (8 H, m, CH_2), 7.28 (6 H, s, Ar−H), 7.30 (12 H, s, Ar−H), 7.93 (2 H, s, Ar−H), 8.10−8.19 (16 H, m, Ar−H), 8.30−8.41 (16 H, m, Ar−H), 8.73 (12 H, s, β-H), 8.83 (6 H, d, J = 5 Hz, β-H), 8.97 (6 H, d, J = 5 Hz, β-H), 8.98 (2 H, d, J = 5 Hz, β-H), 9.13 (2 H, d, J = 5 Hz, β-H), 9.15 (4 H, s, β-H), 10.30 (2 H, s, meso-H), 10.40 (1 H, s CHO); FAB-MS *m*/*z* calcd for $C_{266}H_{224}N_{20}O_1Zn_4$ 3978, obsd 3979 $(M + 1)^+$; UV/vis (CH_2Cl_2) 420, 428, 510, 552, 590, 628 nm.

(41) Yang, S. I.; Lammi, R. K.; Seth, J.; Riggs, J. A.; Arai, T.; Kim, D.; Bocian, D. F.; Holten, D.; Lindsey, J. S. *J. Phys. Chem. A* **1998**, *102*, 9426−9436.

(42) Liddell, P. A.; Kuciauskas, D.; Sumida, J. P.; Nash, B.; Nguyen, D.; Moore, A. L.; Moore, T. A.; Gust, D. *J. Am. Chem. Soc.* **1997**, *119*, 1400−1405.

(F) Hexad 1. Pentad aldehyde **8** (10 mg, 2.5×10^{-6} mol), 10 mg of C_{60} (1.39×10^{-5} mol), 10 mg of sarcosine (1.12×10^{-4} mol), and 5 mL of toluene were warmed to 110 °C under a nitrogen atmosphere for 24 h. Upon cooling, the reaction mixture was diluted with an equal volume of carbon disulfide, applied to a silica gel column, and eluted with a 1:1 mixture of methylene chloride/carbon disulfide to give 8 mg (67% yield) of hexad **1**: ^{1}H NMR (500 MHz, $CDCl_3$) δ −2.42 (1 H, s, NH), −2.40 (1 H, s, NH), 1.17 (12 H, m, CH_3), 1.81 (8 H, m, CH_2), 1.88 (54 H, s, Ar−oCH_3), 2.06 (6 H, s, Ar−oCH_3), 2.26 (8 H, m, CH_2), 2.63 (6 H, s, CH_3, P), 2.64 (6 H, s, CH_3, P), 2.65 (27 H, s, Ar−pCH_3), 3.12 (3 H, s, NCH_3), 4.03 (8 H, m, CH_2), 4.41 (1 H, d, J = 8 Hz, pyrrolid-H), 5.13 (1 H, d, J = 8 Hz, pyrrolid-H), 5.25 (I H, s, pyrrolid-H), 7.26 (6 H, s, Ar−H), 7.28 (12 H, s, Ar−H), 7.87 (2 H, s, Ar−H), 8.04 (4 H, d, J = 8 Hz, Ar−H), 8.08 (6 H, d, J = 8 Hz, Ar−H), 8.13 (6 H, d, J = 8 Hz, Ar−H), 8.16 (4 H, brs, Ar−H), 8.31 (6 H, d, J = 8 Hz, Ar−H), 8.37 (2 H, d, J = 8 Hz, Ar−H), 8.38 (4 H, d, J = 8 Hz, Ar−H), 8.72 (12 H, s, β-H), 8.81 (6 H, d, J = 5 Hz, β-H), 8.96 (6 H, d, J = 5 Hz, β-H), 8.97 (2 H, d, J = 5 Hz, β-H), 9.12 (2 H, d, J = 5 Hz, β-H), 9.14 (4 H, s, β-H), 10.20 (2 H, s, meso-H); MALDI-TOF-MS *m*/*z* calcd for $C_{328}H_{229}N_{21}Zn_4$ 4726, obsd 4727; UV/vis (CH_2Cl_2) 422, 428, 510, 552, 590, 630, 706 nm.

(2) Instrumental Techniques. The ^{1}H NMR spectra were recorded on Varian Unity spectrometers at 300 or 500 MHz. Unless otherwise specified, samples were dissolved in deuteriochloroform with tetramethylsilane as an internal reference. Mass spectra were obtained on a Kratos MS 50 mass spectrometer operating at 8 eV in FAB mode or a matrix-assisted laser desorption/ionization time-of-flight spectrometer (MALDI-TOF), as indicated. Ultraviolet/visible spectra were measured on a Shimadzu UV2100U UV/Vis Spectrometer, and fluorescence spectra were measured on a SPEX Fluorolog using optically dilute samples and corrected. All fluorescence emission quantum yields were determined by the comparative method using toluene solutions of 5,10,15,20-tetraphenylporphyrin (Φ_f = 0.11) as a standard.

Fluorescence decay measurements were performed on $\sim 1 \times 10^{-5}$ M solutions by the time-correlated single photon counting method. The excitation source was a cavity-dumped Coherent 700 dye laser pumped by a frequency-doubled Coherent Antares 76s Nd:YAG laser.[43] The instrument response function was 35 ps, as measured at the excitation wavelength for each decay experiment with Ludox AS-40.

Nanosecond transient absorption measurements were made with excitation from an Opotek optical parametric oscillator pumped by the third harmonic of a Continuum Surelight Nd:YAG laser. The pulse width was ~5 ns, and the repetition rate was 10 Hz. The detection portion of the spectrometer has been described elsewhere.[44]

The femtosecond transient absorption apparatus consisted of a pulsed laser source and a pump−probe optical setup. The laser pulse train was provided by a Ti:Sapphire regenerative amplifier (Clark-MXR, Model CPA-1000) pumped by a diode-pumped CW solid-state laser (Spectra Physics, Model millennia V). The typical laser pulse was 100 fs at 790 nm, with a pulse energy of 0.9 mJ at a repetition rate of 1 kHz. Most of the laser energy (90%) was used to pump an optical parametric amplifier (Clark-MXR IR−OPA). For 560 nm excitation, the OPA was modified to generate output through frequency mixing, with a typical pulse energy of 10−30 μJ. For 398 nm excitation, the second harmonic of the fundamental wavelength was used. The excitation beam was sent through a computer-controlled delay line and used as the excitation pulse. The rest of the laser output (10%) was focused into a 1.2 cm rotating quartz plate to generate a white light continuum. The continuum beam was further split into two identical parts, which were used as the probe and reference beams. The probe and reference signals were focused into two separated optical fiber bundles coupled to a spectrograph (Acton Research SP-275). The spectra were acquired on a dual diode array detector (Princeton Instruments DPDA-1024).[45]

For 590 nm excitation experiments, the laser pulse train was provided by a single jet ultra short pulse dye laser (Spectra Physics 3500) synchronously pumped by a frequency-doubled, mode locked CW Nd:YAG laser (Spectra Physics 3800). Both laser pulse trains were compressed using fiber compression techniques (Spectra Physics CP-1 and 3695 pulse compressors). The laser pulse was then amplified by a three-stage picosecond tunable dye amplifier (Continuum PTA-1000) pumped by a high repetition rate regenerative amplifier (Continuum RGA-1000). The final output pulses from the laser and amplified system were 100−200 fs full width at half-maximum at 590 nm, 200 μJ, and produced at a repetition rate of 540 Hz. The spectrometer and detection system was as described above, except that the white light continuum was generated in a 1 cm water flow cell.[46]

To determine the number of significant components in the transient absorption data, we carried out singular value decomposition analysis[23,24] using locally written software based on the MatLab 5.0 program (MathWorks, Inc.) Decay-associated spectra were obtained by fitting the transient absorption change curves over a selected wavelength region simultaneously as described by eq 12, where $\Delta A(\lambda,t)$ is the observed

$$\Delta A(\lambda,t) = \sum_{i=1}^{n} A_i(\lambda) \exp(-t/\tau_i) \qquad (12)$$

absorption change at a given wavelength at time delay t and n is the number of kinetic components used in the fitting. A plot of $A_i(\lambda)$ versus wavelength is called a decay-associated spectrum and represents the amplitude spectrum of the ith kinetic component, which has a lifetime of τ_i.

Acknowledgment. This work was supported by grants to D.G. and T.A.M. from the National Science Foundation (CHE-9709272) and to J.S.L. from the Department of Energy, Office of Basic Energy Sciences. FAB mass spectrometric studies were performed by the Midwest Center for Mass Spectrometry, with partial support by the National Science Foundation (DIR9017262). This is publication 412 from the ASU Center for the Study of Early Events in Photosynthesis.

JA991255J

(43) Gust, D.; Moore, T. A.; Luttrull, D. K.; Seely, G. R.; Bittersmann, E.; Bensasson, R. V.; Rougée, M.; Land, E. J.; de Schryver, F. C.; Van der Auweraer, M. *Photochem. Photobiol.* **1990**, *51*, 419−426.

(44) Davis, F. S.; Nemeth, G. A.; Anjo, D. M.; Makings, L. R.; Gust, D.; Moore, T. A. *Rev. Sci. Instrum.* **1987**, *58*, 1629−1631.

(45) Freiberg, A.; Timpmann, K.; Lin, S.; Woodbury, N. W. *J. Phys. Chem. B* **1998**, *102*, 10974−10982.

(46) Lin, S.; Chiou, H.-C.; Kleinherenbrink, F. A. M.; Blankenship, R. E. *Biophys. J.* **1994**, *66*, 437−445.